$$0 = -\frac{1}{\rho r}\frac{\partial}{\partial \varphi}\left(p + \frac{B^2}{2\mu_0}\right) + 2\frac{\nu}{r^3}\frac{\partial f}{\partial \varphi} \qquad (12)$$

However, as shown in Refs 1 and 3, f is essentially independent of φ except very near the radial vane surface Hence, as a first approximation, one may assume that f is independent of φ This is equivalent to assuming that all viscous effects are confined to the boundary layer near the vane surface

With f a constant, the velocity is independent of φ, and it can be shown that the magnetic field is also independent of φ Elimination of **J** from Eqs (3) and (6), taking the curl of the resulting expression, and utilizing Eq (5) yields

$$\nabla^2\mathbf{B} + \mu_0\sigma\nabla \times (\mathbf{V} \times \mathbf{B}) = 0 \qquad (13)$$

By use of the previously stated assumptions, Eq (13) reduces to

$$\frac{d^2B}{dr^2} + \frac{1}{r}\frac{dB}{dr} - \frac{\mu_0\sigma f}{r}\frac{dB}{dr} = 0 \qquad (14)$$

Reference 4 shows that $f = -r|u_{\max}|$ Let $r = \xi L$, and define a magnetic Reynolds number by[1 3]

$$R_m = \mu_0\sigma|u_{\max}|L \qquad (15)$$

Then Eq (14) becomes

$$\frac{d^2B}{d\xi^2} + \left(\frac{1}{\xi} + R_m\right)\frac{dB}{d\xi} = 0 \qquad (16)$$

Integrating once with the boundary condition[1] that at $\xi =$ 1 0

$$dB/d\xi = -R_mB_0$$

where B_0 is the initially applied magnetic field, one obtains

$$dB/B_0 = -(R_m/\xi)e^{Rm(1-\xi)}\,d\xi \qquad (17)$$

The solution of this equation,[5] with the boundary condition that $B = B_0$ at $\xi = 1\ 0^1$, is

$$B/B_0 = 1 + [Ei(-R_m) - Ei(-R_m\xi)]R_me^{R_m} \qquad (18)$$

Equation (18), which is a much simpler expression than that given in Refs 1 and 3, is valid for all magnetic Reynolds numbers and involves no more work than looking up previously tabulated functions (e g , Ref 6)

Results and Discussion

The magnetic field ratio for several magnetic Reynolds numbers is shown in Fig 2 as a function of the ratio of the inner to outer radius of the annulus The results of Refs 2 and 3 also have been included for comparison The R_m = 0 8, 1 0, and 2 0 curves were computed by numerical methods,[2] while the R_m = 0 2 and 0 6 curves were obtained by an analytic solution[3] involving a series expansion in R_m Note that the simple approximate solution given by Eq (18) is in good agreement with the results of Ref 2, as well as those of Ref 3 for small R_m The results of Ref 3 diverge considerably from Eq (18) with increasing R_m However, as noted previously, Eq (18) is valid for all R_m, whereas the results of Ref 3 are not Thus, Fig 2 shows that the solution given by Ref 3 is apparently limited to very small values of magnetic Reynolds number

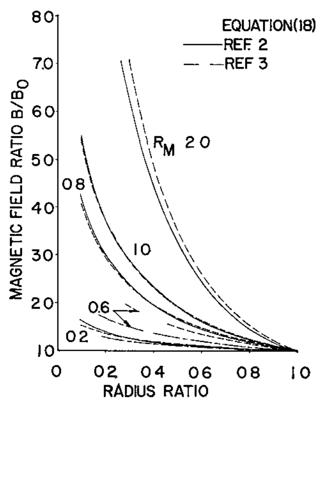

Fig 2 Magnetic field ratio

It is seen in Fig 2 that quite substantial increases in magnetic field can be obtained, even with a small-sized device and with rather low fluid velocities Assuming that the conducting fluid is liquid sodium, that $u_{\max}$ = 0 3 m/sec, and that L = 0 3 m, R_m is approximately 1 1 The corresponding conventional Reynolds number is approximately 4 4 × 10^5, indicating that the viscous effects are indeed confined to a thin layer near the vane surface The limits on generated fields, as well as practical considerations such as viscous and ohmic dissipation, are discussed in Ref 3

After this work was nearly completed, it was discovered that the same inviscid approximation as that above had been made in Ref 7, leading to an equation identical to Eq (16) In Ref 7, however, a solution was obtained using the boundary condition that *all* magnetic flux lines were limited to the region inside the outer radius of the annulus For large R_m, this would lead to prohibitively large current densities in a narrow region near the inner radius The boundary condition used in Refs 1 and 3, as well as in the present work, is that the magnetic field at the outer radius is equal to the applied field This implies that the magnetic flux lines return in a region exterior to the hydromagnet annulus, thereby reducing the possibility of large current densities near the inner radius It should be pointed out that the latter boundary condition also was used in Ref 7 to obtain a solution (identical to Refs 1 and 3) for the case including viscous effects

References

[1] Mawardi, O K , "On a hydro-electromagnet," ARS Paper 1140-60 (May 9–12, 1960)

[2] Schneiderman, A M and Vaughn, L B , "Numerical analysis of a hydro electromagnet," M S Thesis, Mass Inst Tech , Cambridge, Mass (June 1960)

[3] Kolm, H H and Mawardi, O K , "Hydromagnet: a self generating liquid conductor electromagnet," J Appl Phys **32,** 1296–1304 (1961)

[4] Goldstein, S , *Modern Developments in Fluid Dynamics* (Clarendon Press, Oxford, England, 1938), Vol I, pp 106–109

[5] Grobner, W and Hofreiter, N , *Integraltafel, Erster Teil* (Springer-Verlag, Berlin, Germany, 1957), p 108

[6] Jahnke, E , and Emde, F , *Tables of Functions* (Dover Publications, Inc New York, 1945), pp 1–9

[7] Mawardi, O K , "Flux concentration by hydromagnetic flow," *High Magnetic Fields*, edited by H Kolm and B Lax (MIT Press, Cambridge, Mass and John Wiley & Sons, Inc , New York, 1962), Chap 24

Orbital Transfer with Minimum Fuel

W E Bleick* and F D Faulkner†
U S Naval Postgraduate School, Monterey, Calif

A NOTE in this Journal[1] discussed the problem of scheduling the direction p of constant momentum thrust of a rocket, which loses mass at a constant rate, so that it trans-

Received September 18, 1963 This work was supported by the Office of Naval Research Aid of the Computer Facility, U S Naval Postgraduate School, is acknowledged

* Professor, Department of Mathematics and Mechanics
† Professor, Department of Mathematics and Mechanics Member AIAA

fers to a known earth satellite orbit in minimum time T after launching A numerical solution was obtained, using rectangular coordinates, for the case of fixed launching conditions The method of Ref 1 is extended here to solve the problem of orbital transfer of such a rocket with minimum fuel consumption All of the symbols, units, and end conditions of Ref 1 are used here without redefinition

Statement of the Problem

The time of flight T in minimum fuel transfer must be longer than in the minimum time transfer of Ref 1, unless these two trajectories turn out to be identical This implies at least one interruption in rocket thrust during mini num fuel transfer The problem solved here assumes exactly one such interruption, i e , launch at $t = 0$, thrust interruption at $t = t_1$, thrust resumption at $t = t_2$, and final thrust termination at transfer $t = T$ The problem of minimum fuel transfer is equivalent to the Lagrange calculus of variations problem of requiring the integral

$$J = \int_0^T (f + \lambda\varphi_1 + \mu\varphi_2 + \pi\varphi_3 + \rho\varphi_4)dt \qquad (1)$$

to be stationary, where f is the fuel consumption rate, λ,μ,π,ρ are continua of Lagrangian multipliers, and $\varphi_1 = \varphi_2 = \varphi_3 = \varphi_4 = 0$ are the first order equations of rocket motion of Ref 1 The f function and the rocket thrust per unit remaining mass function a are defined as follows: For $0 < t < t_1, f = 1$ and $a = c\dot{M}/(1 - \dot{M}t)g$ For $t_1 < t < t_2, f = 0$ and $a = 0$ For $t_2 < t < T, f = 1$ and $a = c\dot{M}/[1 - \dot{M}(t + t_1 - t_2)]g$ Note that, for $t_2 < t < T, \partial a/\partial t_1 = -\partial a/\partial t_2 = ga^2/c$ The varied time subinterval endpoints in Eq (1) are taken as $t_1 + \Delta t_1$, $t_2 + \Delta t_2$, and $T + \Delta T$ The vanishing first variation δJ and its partial integration are computed as in Ref 1 The coefficients of $\delta u,\delta v,\delta x,\delta y,\delta p$ in $\delta J = 0$ give the Euler equations (2) and (3), consisting of the adjoint equations

$$\begin{aligned} \dot{\lambda} + \pi = 0 \qquad & \mu + \rho = 0 \\ \dot{\pi} + g_{1x}\lambda + g_{2x}\mu = 0 \qquad & \dot{\rho} + g_{1y}\lambda + g_{2y}\mu = 0 \end{aligned} \qquad (2)$$

and the control equation

$$\tan p = \mu/\lambda \qquad (3)$$

The coefficient of ΔT in $\delta J = 0$ gives, with the aid of Eq (3), the transversality condition

$$(\mathbf{a}\ \mathbf{\Lambda})_T = (a\Lambda)_T = 1 \qquad (4)$$

where the adjoint vector $\mathbf{\Lambda} = \mathbf{i}\lambda + \mathbf{j}\mu$, $\Lambda = |\mathbf{\Lambda}| = (\lambda^2 + \mu^2)^{1/2}$, and $\mathbf{a} = a(\mathbf{i}\cos p + \mathbf{j}\sin p)$ The coefficients of Δt_1 and Δt_2 in $\delta J = 0$ give, with the aid of Eq (4), the corner conditions

$$H(t_1) = [a\Lambda]_{t_1}{}^T - \frac{g}{c}\int_{t_1}^T a^2\Lambda dt = 0 \qquad H(t_2) = 0 \qquad (5)$$

Equations (5) are equivalent, by the definition of a, to

$$\Lambda(t_1) = \Lambda(t_2) \qquad (6)$$

and, by partial integration, to

$$\int_{t_2}^T a\dot{\Lambda}dt = 0 \qquad (7)$$

Numerical Solution

Let λ_i, μ_i, π_i, ρ_i, $i = 1, 2, 3, 4$ be four linearly independent solutions of the adjoint Eqs (2) corresponding to the columns of the matrix $\mathbf{E}(t)$ of Ref 1 The control angle p of Eq (3) is defined by

$$\tan p = (\mu_1 + l\mu_2 + m\mu_3 + n\mu_4)/(\lambda_1 + l\lambda_2 + m\lambda_3 + n\lambda_4) \qquad (8)$$

and its variation δp is obtained in terms of δl, δm, δn by total differentiation [1] The Bliss fundamental formulas are obtained by assuming that a solution of the rocket motion equations $\varphi_1 = \varphi_2 = \varphi_3 = \varphi_4 = 0$ has been found, corresponding to Eq (8), which does not necessarily satisfy the terminal conditions at $t = T$ or the corner condition, Eqs (5) By using this solution and holding T fixed, but allowing t_1 and t_2 to vary, find the variation of the vanishing matrix integral

$$\int_0^T [\varphi_1,\varphi_2,\varphi_3,\varphi_4]\mathbf{E}(t)dt = 0 \qquad (9)$$

with the terminal constraints at $t = T$ removed Since the columns of $\mathbf{E}(t)$ satisfy the adjoint Eqs (2), one obtains the system of Bliss formulas in the 1×4 matrix equation

$$[\delta u,\delta v,\delta x,\delta y]_T\mathbf{E}(T) + [\mathbf{G}(t_1) - (a\mathbf{pF})_T]\Delta t_1 - [\mathbf{G}(t_2) - (a\mathbf{pF})_T]\Delta t_2 = [0,\delta l,\delta m,\delta n]\mathbf{A} \qquad (10)$$

where the matrix $\mathbf{A}$ has been defined in Ref 1, and where the matrix

$$\mathbf{G}(t) = (a\mathbf{pF})_t{}^T - \frac{g}{c}\int_t^T a^2\mathbf{pF}dt \qquad (11)$$

where the 2×4 matrix $\mathbf{F}(t)$ is the first two rows of $\mathbf{E}(t)$, and where the matrix $\mathbf{p} = [\cos p, \sin p]$ Substitution of

$$[\delta u,\delta v,\delta x,\delta y]_T = [U - u,V - v,X - x,Y - y]_T + [\dot{U} - \dot{u},\dot{V} - \dot{v},\dot{X} - \dot{x},\dot{Y} - y]_T\Delta T \qquad (12)$$

into Eq (10) gives four of the required six Newton-Raphson equations for the determination of $\Delta T,\Delta t_1,\Delta t_2,\delta l,\delta m,\delta n$ on the varied trajectory The remaining two equations attempt to satisfy the corner condition, Eqs (5), on the varied trajectory Involved here are the differentials

$$\begin{aligned} da &= \delta a + \dot{a}dt \\ &= (\partial a/\partial t_1)\Delta t_1 + (\partial a/\partial t_2)\Delta t_2 + (ga^2/c)dt \end{aligned} \qquad (13)$$

and

$$\begin{aligned} d\Lambda &= \delta\Lambda + \dot{\Lambda}dt \\ &= [0,\delta l,\delta m,\delta n]\mathbf{F}'\mathbf{p}' + (\dot{\lambda}\cos p + \dot{\mu}\sin p)dt \end{aligned} \qquad (14)$$

where the primes on $\mathbf{F}$ and $\mathbf{p}$ indicate matrix transposition Use of Eqs (6) and (14) yields the Newton-Raphson equation

$$\dot{\Lambda}(t_1)\Delta t_1 - \dot{\Lambda}(t_2)\Delta t_2 - [0,\delta l,\delta m,\delta n][\mathbf{F}'\mathbf{p}']_{t_1}{}^{t_2} = \Lambda(t_2) - \Lambda(t_1) \qquad (15)$$

Use of Eqs (13) and (14), and the first of Eqs (5), yields the Newton-Raphson equation

$$(a\dot{\Lambda})_T\Delta T + (K - a\dot{\Lambda})_{t_1}\Delta t_1 - K(t_2)\Delta t_2 + [0,\delta l,\delta m,\delta n]\mathbf{G}'(t_1) = -H(t_1) \qquad (16)$$

where

$$K(t) = \frac{g}{c}[a^2\Lambda]_t{}^T - 2\left(\frac{g}{c}\right)^2\int_t^T a^3\Lambda dt \qquad (17)$$

The iteration to successive varied trajectories, using Eqs (10, 12, 15, and 16), may be carried out as in Ref 1 Two devices were used to stabilize the course of the iteration The first was to adjust the m and n values of the new T,t_1,t_2,l,m,n sextuple, found by solving the Newton-Raphson equations, to satisfy the corner condition Eqs (5) before proceeding with the next iteration The second device was to

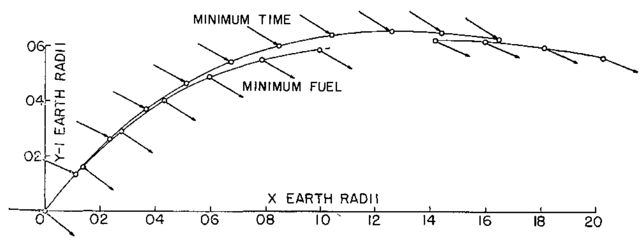

Fig 1 Trajectories and thrust directions

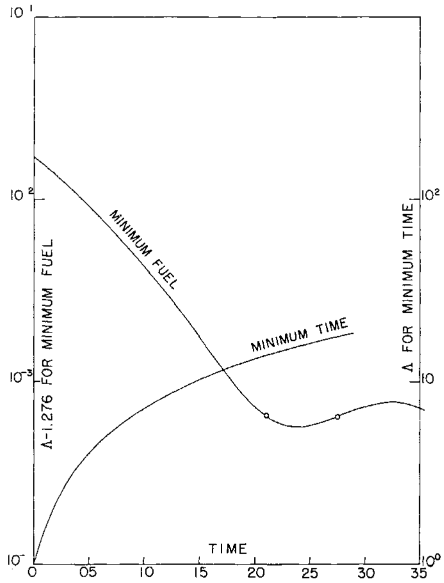

Fig 2 Λ vs time

modify the $[\dot{U},\dot{V},U,V,X,Y]_T$ terms in the Newton-Raphson equations before solving these equations, so as to minimize the sum of the squares of the elements of $[U - u, V - v, X - x, Y - y]_T$

The numerical example of minimum fuel transfer given here involves the same launching conditions, mass loss parameters, and circular orbit used in the minimum time transfer of Ref 1 The results for minimum fuel transfer are $T = 0\ 353977$, $t_1 = 0\ 210293$, $t_2 = 0\ 275349$, $l = -0\ 820196$, $m = -0\ 708727$, $n = -1\ 181390$, and the transfer sector angle $B = 0\ 189345$ rad Since the minimum time trajectory of Ref 1 gave $T = 0\ 289869$, the net fuel saving in minimum fuel transfer over minimum time transfer is measured by $0\ 289869$–$0\ 353977 + t_2 - t_1 = 0\ 000948$, or an unspectacular $\frac{1}{3}\%$ Figure 1 shows the trajectories and thrust directions for minimum time and minimum fuel transfer

The semilogarithmic plots of Fig 2 show the different behavior of Λ vs time in the two problems For some reason there is a much greater difference than expected The curve increases monotonically for minimum time transfer The curve for minimum fuel shows a rather characteristic shape It is initially large and decreasing; it then increases, and then decreases If the final decreasing interval does not occur, larger values of T lead to lower values of fuel consump tion, as may be partially inferred from Eq (7)

Reference

[1] Bleick, W E, "Orbital transfer in minimum time," AIAA J 1, 1229–1231 (1963)

Hypersonic Blunt-Body Flow Fields at Angle of Attack

RUDOLPH J SWIGART*
Lockheed Missiles and Space Company, Huntsville, Ala

I Introduction

A NEW method of solving the supersonic blunt-body problem has been developed recently by the author [1] This method has proved to be as accurate as other methods in popular use for calculating plane-symmetric and axisymmetric flow in the subsonic portion of the shock layer, and has the additional advantage of being readily extendable to the calculation of flows about blunt-nosed configurations at angle of attack

The method is an inverse one, that is, the freestream conditions and shape of the detached shock wave are taken as known, and the body shape and flow field are to be determined The success of the method rests with the rapid convergence of assumed power-series expansions for certain flow variables about the shock-wave axis of symmetry and about zero angle of attack Only first order terms in angle of attack are retained Substitution of these series into the governing differential equations and boundary conditions reduces the problem to integration of ordinary differential equations that determine the series coefficients The integration can be performed by truncating the series about the shock-wave axis of symmetry at any desired number of terms

Reference 1 contains results for flow past inclined blunt bodies for two shock-wave shapes at infinite freestream Mach numbers In that report, attention is focused on the question of whether or not the streamline that wets the body in asymmetric flow is the one that crosses the shock at right angles and hence has maximum entropy in the shock layer It is pointed out that, in a properly posed method of analysis, no assumption regarding the behavior of the maximum-entropy streamline is required Consideration of flow past bodies supporting parabolic (two-dimensional) and paraboloidal (three-dimensional) shock waves at positive angle of attack leads to the conclusion that the maximum-entropy and body streamlines are not one and the same, the maximum-entropy streamline passing slightly below the body in both cases In Part I of Ref 1, prior solutions to the asymmetric problem by other investigators are discussed, and it is noted that these solutions depend upon the assumption that the body is wetted by the streamline of maximum entropy Indeed, even in work published more recently than Ref 1, this assumption is still being made [2]

Subsequent to the work described in Ref 1, the algebra involved has been carried out for obtaining results from the theory of that reference for inclined bodies of arbitrary shape (with the not too confining restriction that these bodies support shock waves that are conic sections) at arbitrary freestream Mach number Two computer programs have been developed, one to calculate asymmetric flow past inclined two-dimensional bodies, and the other to handle three-dimensional flow past inclined bodies supporting axisymmetric shock waves

Several results of these computer programs are presented in this note A critical appraisal is made of the error involved in neglecting second and higher-order terms in the angle-of-attack series by considering flow past circular and spherical shock waves at freestream Mach numbers of infinity and 4 0 Since the flow past a circular or spherical shock wave at angle should be the same as the flow past these same shock waves at zero angle and rotated through the angle of attack, comparison with rotated zero-angle solutions provides an index of the error generated by neglecting higher-order terms Flow past a 3:2 axis-ratio prolate ellipsoid of revolution at 7 5° angle of attack is also considered, and results for the surface pressure distribution in the vertical symmetry plane are compared with the experiment

II Analysis

The details of analysis of asymmetric blunt-body flows by the method of series expansion about the shock-wave axis of symmetry and about zero angle of attack are given in Ref 1 Equations (8a, 8b, 9a, 10a, and 11) of that report govern two-dimensional asymmetric flow The boundary conditions at the shock wave and explicit expression for the function $f(\psi)$ [Eqs (9a) and (10a) of Ref 1], are derived in Appendix I of Ref 3 The differential equations governing

---

Received September 19, 1963
* Head Theoretical Fluid Mechanics Research